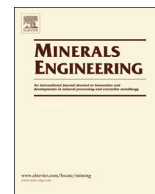




ELSEVIER

Contents lists available at ScienceDirect

Minerals Engineering

journal homepage: www.elsevier.com/locate/mineng

Seawater flocculation of clay-based mining tailings: Impact of calcium and magnesium precipitation



Jahir J. Ramos^a, Williams H. Leiva^b, Claudia N. Castillo^{c,d}, Christian F. Ihle^{c,e}, Phillip D. Fawell^f, Ricardo I. Jeldres^{a,*}

^a Departamento de Ingeniería Química y Procesos de Minerales, Facultad de Ingeniería, Universidad de Antofagasta, PO Box 170, Antofagasta, Chile

^b Faculty of Engineering and Architecture, Universidad Arturo Prat, Almirante Juan José Latorre 2901, Antofagasta, Chile

^c Laboratory for Rheology and Fluid Dynamics, Department of Mining Engineering, Universidad de Chile, Beauchef 850, 8370448 Santiago, Chile

^d CSIRO Mineral Resources, Santiago, Chile

^e Advanced Mining Technology Center, Universidad de Chile, Tupper 2007, 8370451 Santiago, Chile

^f CSIRO Mineral Resources, Waterford, Western Australia, Australia

ARTICLE INFO

Keywords:

Seawater flocculation

Mining waste

Clay-based tailing

Polyacrylamide

Hydrolyzed magnesium complex

ABSTRACT

In areas where access to water of good quality is limited, the use of seawater in mineral processing can be an option. However, the dewatering of waste tailings is adversely affected, particularly when this follows processing at higher pH. The flocculation response of a synthetic clay-based tailings in seawater to different pH conditions was examined in detail, focusing on conditions promoting precipitation of the divalent cations present. Flocculated aggregate growth and breakage during turbine mixing were monitored in-situ in terms of chord length distributions (by focused beam reflectance measurement) and aggregate image capture, with the resultant hindered settling rates also determined. It was found that flocculation in seawater was substantially impaired at pH values greater than 10.3 due to the precipitation of magnesium species. The addition of the precipitated phase to the synthetic tailings increases both the surface area exposed to flocculant and the number of particles or micro-aggregates then needing further aggregation to attain acceptable settling rates. The direct use of seawater in processing operations without resorting to full desalination does not necessarily have detrimental impacts on tailings flocculation and thickening, provided the operation is conducted at a pH that prevents the precipitation of magnesium present within the process liquors.

1. Introduction

It is increasingly common to find industrial operations that use seawater directly in the processing of minerals, with numerous examples in flowsheets for the recovery of zinc, uranium, iodine and copper (Cisternas and Gálvez, 2018). Although its implementation can involve several operational challenges and require changes in infrastructure, in some areas where water is scarce, seawater becomes the only viable option to preserve the industry's sustainability (Cisternas and Gálvez, 2018; Jeldres et al., 2016; Ordóñez et al., 2013). Mining in desert areas often coincides with long distances from water sources and, in the Chilean context, also operating at high altitudes, which introduces pumping costs that may become significant (Ihle and Kracht, 2018). It is therefore essential to rely on cost-efficient water recovery processes to minimize energy demand.

As a consequence, gravity thickening unit operations acquire a

crucial role within operating flowsheets, since it is within the tailings circuit where the highest amount of water is recovered and returned to the process. Solid-liquid separation by gravity sedimentation is enhanced by aggregating fine particles within dilute tailings feed suspensions, forming beds within the thickener from which a concentrated underflow solid suspension can be removed from below, while clarified liquor is collected at the peripheral overflow.

The formation of aggregates in thickeners is promoted by dosing with flocculants, which are long-chain water soluble polymers of high molecular weight. Industrial tailings operations typically use hydrolysed polyacrylamides (HPAM) of varying anionic charge densities. In this context, polymer bridging is the major mechanism by which polymer can destabilize solid particles in suspension. Over the typical pH range for tailings, polymer adsorbs onto neutral surface sites on the particles through hydrogen bonding by amide functionalities (Hocking et al., 1999). By this mechanism, some segments of the long-chain

* Corresponding author.

E-mail address: ricardo.jeldres@uantof.cl (R.I. Jeldres).

<https://doi.org/10.1016/j.mineng.2020.106417>

Received 2 January 2020; Received in revised form 28 April 2020; Accepted 30 April 2020

Available online 06 May 2020

0892-6875/ © 2020 Elsevier Ltd. All rights reserved.

polymer become attached to different particles to bridge between them, and under the appropriate conditions can form large but highly porous and fragile aggregates that settle rapidly. The anionic carboxylate ($-\text{COO}^-$) functionality promotes chain extension in solution, increasing the probability of bridging adsorption, and avoiding too much attachment onto the same particle.

When the feed suspension contains significant sub-micron particles, the flocculant dosages required can become prohibitive (Hogg, 1999), in which case pre-dosing with a coagulant is recommended. Coagulants are inorganic cations or charged short-chain polymers that can adsorb on surfaces and favour charge-based aggregation; the aggregate sizes formed may be small, but are sufficient to reduce subsequent flocculant dosing requirements.

There is currently limited definitive information on the impact of seawater on gravity thickener performance; in contrast, there is considerable evidence related to the influence of salinity on the flocculation process, although much of it can appear on first pass to be contradictory. For example, Liu et al. (2018) reported that high-salinity water assisted bentonite and illite to settle faster through improved aggregation but hindered the settling rate of kaolinite. Others have described where high salinity adversely impacts on aggregate formation (Costine et al., 2018; Ji et al., 2013; Lee et al., 2012; Witham et al., 2012). Jeldres et al. (2017c) indicated that the influence of salinity on the size of aggregates formed from polymer-bridging flocculation is complex due to a number of competing effects. A highly saline medium favors interactions between the polyelectrolyte and quartz that are much less likely to occur at a very low ionic strength. Cations in solution shield the $-\text{COO}^-$ functionalities of HPAM and they also adsorb onto the mineral surface; together this enables a greater proportion of HPAM functionalities to approach closer to the surface and promote adsorption by both hydrogen bonding and cationic bridging. At the same time, the shielding of the charged HPAM functionalities at high salinity causes the flocculant chain to take a much less extended conformation in solution, thus limiting the bridging capacity of the adsorbed chains and the size of aggregates that can then be formed. These competing effects were demonstrated through molecular simulations for the interaction of an HPAM with a quartz surface, varying the salt concentration (Quezada et al., 2018).

For suspensions in seawater, it is not just the ionic strength that influences flocculation. There are also significant concentrations of calcium and magnesium cations, which raises the prospect of forming $\text{Ca}(\text{OH})^+/\text{Mg}(\text{OH})^+$ complexes and varied solid substances (e.g. $\text{Ca}(\text{OH})_2$, $\text{Mg}(\text{OH})_2$, etc.) (El-Manharawy and Hafez, 2003). These complexes may adsorb onto the mineral's surface, affecting the Cu-Mo flotation stages (Jeldres et al., 2019; Li et al., 2018a, 2017), where the priority is to operate under highly alkaline conditions to boost pyrite depression, given this non-valuable sulfide loses its floatability at $\text{pH} > 10.5$ (Castro, 2018; Li et al., 2018b, 2017; Paredes et al., 2019). For this reason, recent studies propose new strategies for the use of seawater in concentration operations, reducing the magnesium content either with alkalizing agents (Jeldres et al., 2017a) or through a CO_2 -rich atmosphere (Cruz et al., 2019).

In the case of thickening, it is known that multivalent cations have a direct impact on the mechanisms of particle flocculation. For example, Peng and Di (1994) showed that Ca^{2+} and $\text{Ca}(\text{OH})^+$ could interact with the carboxylate groups of HPAMs, forming complexes such as $-(\text{COO})_2\text{Ca}$ or $\text{COOCa}(\text{OH})$. This may reduce the available functional groups of the flocculant and its solution conformation, both potentially detrimental to its bridging capacity. The formation of complex precipitates of calcium and magnesium could also cover the active surface of kaolinite, possibly inhibiting flocculant adsorption. Peng and Di (1994) calculated that the solubility constant produced by the hydrolysis of calcium on the surface of kaolinite is an order of magnitude smaller than that for calcium in solution, which may imply precipitates would have a greater tendency to stay on the solid surface.

Mpofu et al. (2003) found that the zeta potential of kaolinite

particles at $\text{pH} > 9$ in the presence of 10^{-1} M Ca^{2+} switched from negative to positive, interpreted in terms of the adsorption of hydrolyzed calcium species (e.g. $\text{Ca}(\text{OH})^+$) or even $\text{Ca}(\text{OH})_2$ precipitation on the particle surfaces. A similar argument was also made by Atesok et al. (1988) for kaolinite particles. Zbik et al. (2008) used cryo-SEM to show kaolinite initially forms edge-edge (EE) and edge-face (EF) inter-particle associations to give open, loose structures that are largely preserved on flocculation, however, the presence of calcium ions generated aggregates with less elongated structures dominated by EF associations. Jeldres et al. (2017c) suggested the presence of electrolytes is linked to the formation of more compact kaolinite aggregates in comparison with those formed at very low ionic strength. The impact of calcium ions on the rheology of clay suspensions was analyzed by Avadiar et al. (2014), who showed that hydrolyzed calcium complexes adhere to kaolinite surfaces, inducing aggregation and increasing the strength of the suspension structure. The consequence of this phenomenon is a measurable increase in the suspension yield stress under alkaline conditions. They then considered the influence of calcium and magnesium cation hydrolysis on quartz, alumina, and kaolin suspensions, finding the complexes can adhere to the surface of the three minerals, causing a significant rise in zeta potential (Avadiar et al., 2015).

Although the mechanisms by which different types of ions impact upon flocculation of the main minerals within tailings (e.g. quartz and clays) are reasonably well understood (Castillo et al., 2019; Costine et al., 2018; Romero et al., 2018), there has been no systematic study tackling the effect of seawater and divalent ion complexes on aggregation under conditions relevant to feedwell flocculation in an industrial tailings thickener. In this paper, a quartz-kaolin suspension in seawater is used as an analogue for mineral tailings obtained following copper sulphide flotation. The physical response of the suspension (extent of aggregation and zeta potential) was examined over a range of pH values, as well as its flocculation at different solids concentrations. Emphasis is given to conditions that promote the presence of divalent ion complexes. The constituents of the system are also analyzed separately, considering the main divalent cations (Ca^{2+} and Mg^{2+}) that will be present.

2. Materials and methods

2.1. Materials

Quartz-kaolin mineral mixtures were used as a synthetic tailings. The kaolin sample was purchased from a local Chilean store, quantitative XRD analysis showing it contained 93.5 wt% kaolinite and 6.5 wt% quartz. SEM images of the kaolin particles (Fig. 1) display the familiar plate-like structure, with basal and edge faces readily distinguished.

The flocculant used was a commercial anionic polyacrylamide (HPAM), SNF 704. According to the supplier (SNF Chile S.A.), the polymer has a molecular weight $> 18 \times 10^6$ g/mol and a medium charge density (e.g. 30–50% anionic functionalities). Aqueous stock solutions of this powder product were prepared at a concentration of 1 g/L. It was gently mixed for 24 h prior to use and discarded after two weeks to avoid potential aging effects. Once a day, an aliquot of this stock flocculant solution was diluted at 0.1 g/L for use in testing, with unused portions then discarded. Flocculant dosages are expressed in terms of grams of polymer per tonne of dry solids (g/tonne).

Seawater from the coast of Antofagasta (Chile) was used. Concentrations of Na, Mg and Ca cations were determined by atomic absorption spectroscopy, while the argentometric titration method was applied to determine solution chloride (Cl). The results for the collected seawater were 11580 mg/L Na, 1376 mg/L Mg, 400 mg/L Ca, and 19810 mg/L Cl.

In addition of seawater, Ca and Mg solutions in deionized water (specific conductivity $< 2 \mu\text{S}/\text{cm}$ and $\text{pH} 5$ at 25°C) were prepared. Salts used for solution preparation were CaCl_2 and MgCl_2 , all being of

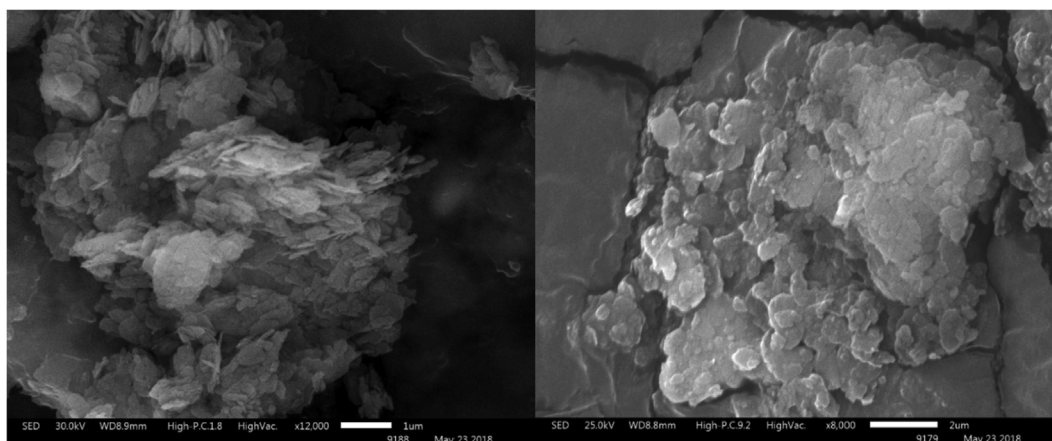


Fig. 1. High-resolution SEM image showing surfaces of kaolin mineral.

analytical reagent grade.

2.2. Particle size distributions

A Malvern Mastersizer 2000 laser diffraction instrument was used to measure volume weighted particle size distributions (PSDs) of solid tailings minerals and precipitated salt phases. Solid samples were suspended in deionized water (specific conductivity < 2 $\mu\text{S}/\text{cm}$ and pH 5 at 25 °C) and dispersed by being held in an ultrasonic bath for 20 min. Knowing that magnesium cations are precipitated as hydroxides when the pH of deionized water was raised to ~ 11 , corresponding precipitates from seawater was formed by adding analytical grade NaOH (solid) with mixing until solid formation was evident (pH ~ 11).

The PSDs for the quartz and kaolin samples (Fig. 2) show that while their median sizes (d_{50}) are similar, the main distinction is in the finer end of the distributions, with d_{10} values of 1.2 and 2.7 μm for kaolin and quartz, respectively. In reality, the primary particle size for kaolin will be much finer, as the larger sizes measured will represent highly agglomerated fines. Full dispersion is not sought in this case, as the clays present within tailings will typically retain some level of agglomeration.

2.3. Zeta potential measurements

Zeta potentials (ZP) for suspended fine particles of quartz and kaolin were measured with a Stabino® (Particle Metrix) instrument that utilizes the streaming potential approach. This instrument has an oscillating piston inside a sample cup (or cell), the piston's motion limiting particle settling during measurements.

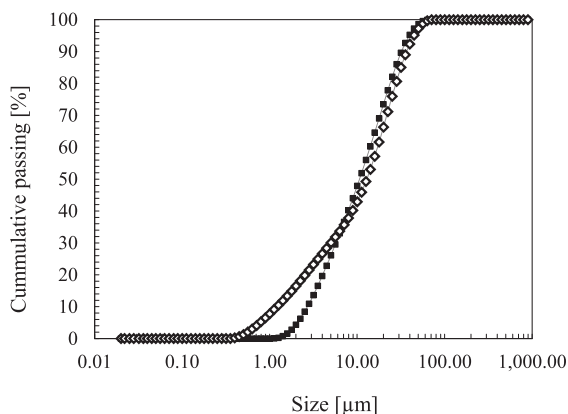


Fig. 2. Particle size distribution of quartz (■) and kaolin (◇) samples in deionized water (obtained by a Malvern Mastersizer 2000 particle analyzer).

To obtain isolated particle ZPs at different pH values, 0.1 wt% solid suspensions in 10^{-3} mol/l NaCl were first made, then pH was adjusted using HCl or NaOH and finally the suspension placed in the Stabino® cell for a 3 min measurement (or until a steady state measurement was achieved).

2.4. Settling tests

The mixing for flocculation experiments was achieved using a 30 mm-diameter PTFE turbine type impeller at the end of a vertical shaft (diameter 4 mm) within a 1 L capacity, 100 mm diameter vessel. In all experiments, the base of the impeller was positioned 20 mm above the vessel's bottom surface. The liquor of interest (232.2 mL) was transferred to the vessel, with known masses of the solid phases then added as dry powders to give mixtures containing 92.3 wt% quartz and 7.7 wt% kaolin at the required total solid concentration and the suspension preconditioned by mixing at 450 rpm for 30 min. After this period, the mixing rate was reduced to 150 rpm, and diluted flocculant was added to give the required dosage, with the mixing maintained for a further 30 s.

Applying the definition for the average velocity gradient (G) in a turbulent regime (Spicer and Pratsinis, 1996), the derived value for G in flocculation experiments at 150 rpm (for the vessel, impeller and conditions described above) was $\sim 163 \text{ s}^{-1}$. Note that the conditions will be expected to produce a distribution of shear rates, and while derived G values may be relevant in low solids wastewater clarification, their significance is less clear in the current application, for which aggregation will take place in low and high shear zones. Previous experiments conducted to identify the best solid-flocculant mixing conditions for this experimental arrangement found that the maximum settling rates were obtained at 150 rpm.

The flocculated suspension was then carefully transferred into a stoppered cylinder (300 cm^3 volume, 35 mm internal diameter), which was inverted twice by hand (the entire cylinder rotation process taking ~ 4 s in all cases) prior to measurement of the batch settling response. The fall of the mudline, defined as the suspension-supernatant interface, was monitored for one hour and the settling rate taken as the initial linear slope of a plot of the mudline height against time.

2.5. Characterization of aggregates: Chord length distribution and images

Real-time monitoring of aggregate formation and size evolution was performed using focused beam reflectance measurement (FBRM) and particle vision measurement (PVM) instruments (both from Mettler Toledo). The FBRM (Particle Track E25) consists of a processing unit and a probe with a 19 mm diameter tip that has a sapphire window (14 mm diameter) at the end. The probe is immersed vertically in the

reaction vessel, 10 mm above the stirrer and 20 mm off-axis. The FBRM probe features a laser that is focused through the sapphire window and scans a circular path at a tangential velocity of 2 m/s; the backscattered light is then received when the laser beam intersects the path of a particle or aggregate. From the duration of any elevated backscattered light intensity and the laser velocity, a chord length is derived. The FBRM software allows the post-processing of the recorded data into histograms of counts corresponding to chord lengths in selected size channels that range from 1 μm to 1 mm as rapidly as every 2 s, and thus temporal progressions within a particle system are readily captured at solids concentrations well above what can be studied by laser diffraction. In this case the chord length distributions (CLDs) represent 100 channels over the full range, but the histograms are presented as line graphs for ease of comparison. Additional details on the technique, together with discussion on its strengths and limitations in flocculation studies, have been published previously (Kyoda et al., 2019).

In selected experiments, a PVM probe (model V819) was substituted for the FBRM probe. The PVM probe also has a tip with a 19 mm outer diameter and a sapphire window through which strobing light sources allow the capture of greyscale images that are $1075 \times 825 \mu\text{m}$ at a resolution of 2 μm . Up to ten images per second can be acquired, but in these experiments a rate of two images per second was chosen.

2.6. Turbidity analysis for precipitate-flocculant interaction

The effectiveness of interactions between flocculant and $\text{Ca}^{2+}/\text{Mg}^{2+}$ hydroxide precipitates was inferred using turbidity measurements of the supernatant solutions from cylinder settling. A set of experiments were conducted with a known volume (38.2 mL) of 0.01 mol/L CaCl_2 and 0.05 mol/L MgCl_2 solutions in deionized water, as well as with seawater, at different pH values (achieved with analytical grade NaOH and HCl). Once the solution was prepared, a 0.1 g/L flocculant solution (1.8 mL) was added and gently mixed for 1 min. Finally the suspensions was allowed to settle in a 50 mL graduated glass cylinder. After 5 min, 4 mL of the supernatant liquid was taken for turbidity analysis, measured (in units of NTU) with a Hach 18900 Turbidity Meter. For baseline experiments, deionized water was used instead flocculant solution.

3. Results and discussion

3.1. Quartz and kaolin zeta potential

Zeta potential measurements were performed on the separate quartz and kaolin suspensions in 10^{-3} mol/L NaCl over a pH range from 2 to 12 (Fig. 3). Both gave an apparent negative zeta potential over most of the pH range, consistent with the expected nature of both minerals (Kaya and Yukselen, 2005). In the case of kaolin, the negative zeta potential reflects the overall magnitude of the combined surfaces of basal and edge faces, indicating the dominance of the negatively charged basal faces. The magnitude of the measured potentials in the alkaline pH range would favour particle dispersion in the absence other added reagents. In seawater, the high salinity makes the zeta potential very low at any pH. Seawater counterions, especially divalent ones like calcium and magnesium, compress the electrical double-layer that surrounds the mineral surfaces. This significantly lowers the range and magnitude of the electrostatic potential.

3.2. Particle aggregation in flocculant-free medium

Studies have shown that hydrolysable species of multivalent metal cations such as Mg^{2+} and Ca^{2+} may adsorb onto mineral surfaces, affecting suspension stability (Manukonda and Iwasaki, 1987; Mpofu et al., 2003). In a flocculant-free system, the presence of such species may favour heterocoagulation of the mineral phases. The ability of FBRM to be applied at practical solids concentrations without the need

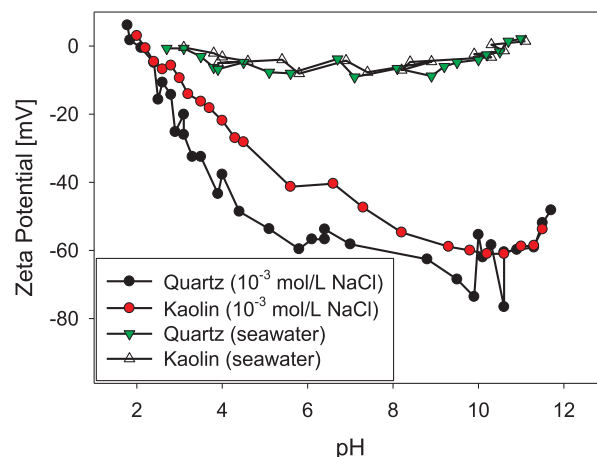


Fig. 3. The zeta potential curves of quartz and kaolin samples in 10^{-3} mol/L NaCl and seawater.

of dilution offers the potential to provide useful insights on the phases present and the extent of aggregation.

Fig. 4 shows the CLDs for the synthetic tailings at pH 8 in both deionised water (DW) and seawater (SW), with the unweighted distributions (Fig. 4A) considered number-sensitive and therefore offering greater sensitivity to changes in the fines region, while the square-weighted distributions (Fig. 4B) reflect a volume-weighting (Heath et al., 2002) and will be more influenced by the contribution of any aggregates formed. The onset of fine particle aggregation from flocculation would normally be expected to induce a shift to the right in both CLDs, as well as a reduction in unweighted peak height and an increase in the volume-weighted peak height (Kyoda et al., 2019). A small shift is evident in the volume-weighted CLD on going from DW to SW, but the response is more complex in the case of the unweighted CLDs, with a decline in counts $> 4 \mu\text{m}$ observed at the same time as an increase in counts $< 4 \mu\text{m}$. Particles $< 1 \mu\text{m}$ will be present in clay suspensions, but are not measured by FBRM – as a consequence, any aggregation of these colloidal particles can then lead to small aggregates being captured in the lowest chord length channels, which can have the effect of lowering the mean or median statistics in the unweighted CLDs. This highlights the importance of always examining the response for both the unweighted and volume-weighted CLDs.

To complement PSD data of the unflocculated particles (Fig. 2), CLDs were measured using solid dispersions in seawater at pH 8 and 11, and in deionized water at pH 8. The unweighted CLDs measured in seawater (Fig. 4A) show a shift in the peak position on increasing the pH from 8 to 11. As discussed above, such a shift is normally considered indicative of greater aggregation of fine particles, but in isolation that would also take place with a significant reduction in the peak height, i.e. the many particles that are captured within a single aggregate then contribute far fewer chord counts to the CLD. With a small decrease in the peak count. While the high salinity of seawater assists towards particle coagulation, through cation adsorption/exchange and double layer compression, it is expected that new complexes and precipitates that form under alkaline conditions (e.g. MgOH^+ , CaOH^+ , $\text{Mg}(\text{OH})_2$) will not only introduce additional particles but further promote particle coagulation. As a consequence, the increase in size observed in Fig. 4A is consistent with aggregation of sub-10 μm particles and micro-aggregates, but an increase in the number of species present above 10 μm .

The PSD of the precipitate formed in seawater at pH 11 was measured to understand possible contribution to the synthetic tailing's PSD under the same conditions. It is interesting to note that the precipitate's PSD (as measured by laser diffraction) had a distinct peak close to 25 μm and only a very minor proportion of submicron solids (Fig. 5).

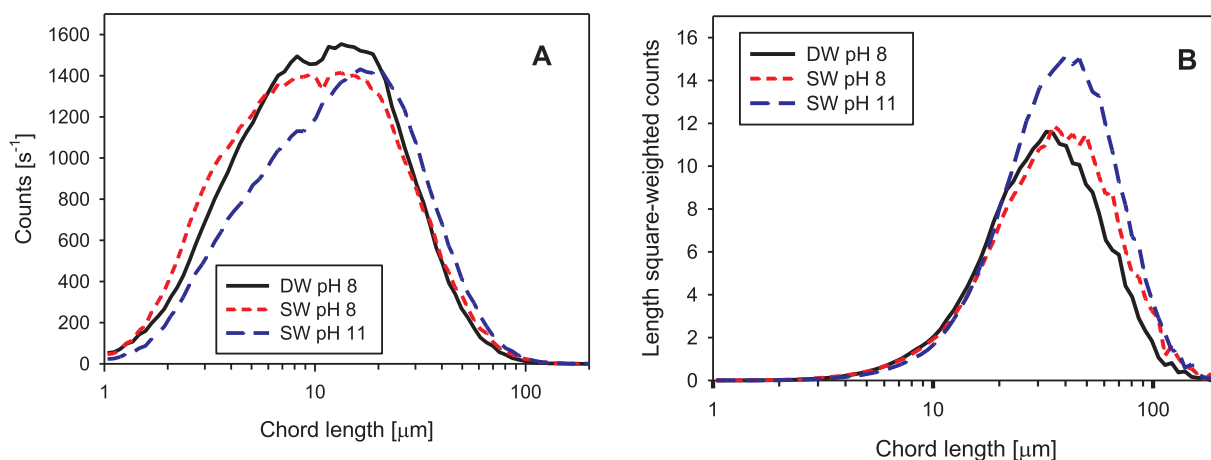


Fig. 4. (A) Unweighted and (B) square-weighted chord length distributions in primary mode for unflocculated 5 wt%, synthetic tailings in seawater (pH 8 and 11) and deionised water (pH 8).

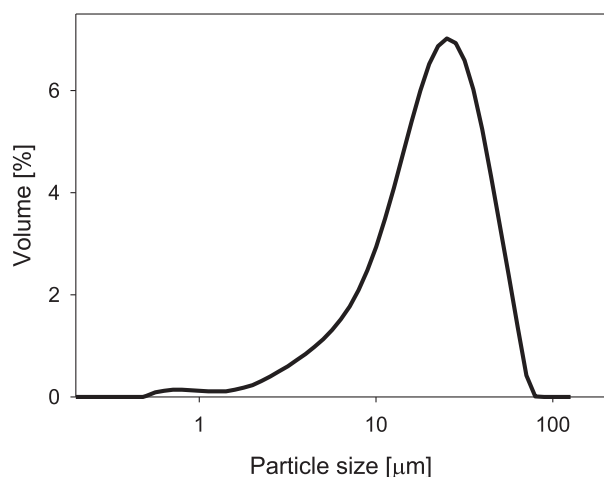


Fig. 5. Size distribution of the precipitate formed in seawater (11,580 mg/L Na, 1376 mg/L Mg, 400 mg/L Ca, and 19,810 mg/L Cl) after the pH adjusted to 11 with NaOH (PSD obtained with a Malvern Mastersizer 2000).

The square-weighted CLDs in seawater (Fig. 4B) confirmed that the rise in pH resulted in an increase in the number of coagulated aggregates, but there was not a significant shift to larger aggregates than those already present at pH 8 (i.e. the peak size remains ~ 25 μm). This is consistent with coagulated aggregates being intrinsically quite weak, with only small sizes thereby formed when under applied turbulence. However, aggregation behaviour was substantially different after the addition of polyelectrolyte, particularly in response to changes in pH, as is explored in the subsequent sections.

3.3. Settling rate at varied pH

The minimum diameter of a gravity thickener requires the liquor rise rate (i.e. the upflow velocity of the released supernatant) to be less than the solids settling rate, with a scale-up factor usually applied to the latter to account for variables such as cross-currents and non-uniform distribution of particles across the thickener diameter (Bedell et al., 2015). The initial settling rate derived from batch testing is therefore an important measure in sizing thickening operations, but it also helps towards understanding how thickener performance is then affected by the operating variables, such as pH, flocculant dosage or solids concentration.

Fig. 6 shows the effect of pH on the measured settling rate of

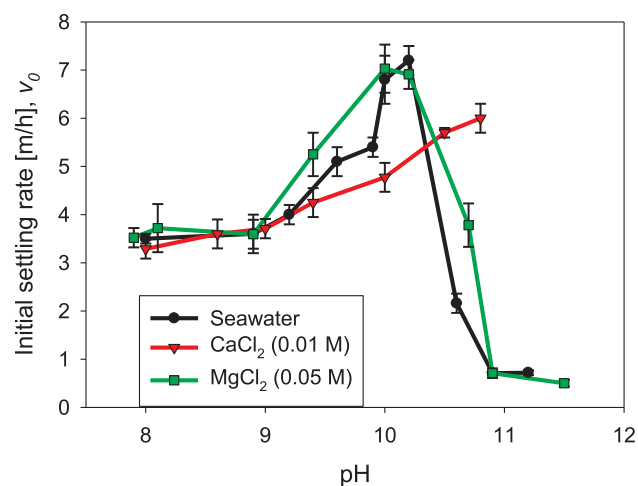


Fig. 6. Settling rate of synthetic tailing flocculated with HPAM in different aqueous media as a function of pH (solid concentration 8 wt%, flocculant dosage 13 g/tonne).

synthetic tailings in different liquors at a fixed flocculant dosage of 13 g/tonne (an arbitrary value chosen to within the typical dosage range used in copper tailings thickening). The tests were carried out with the tailings made-up in three different liquors - seawater, 0.05 M MgCl₂ or 0.01 M CaCl₂. Flocculated settling rates in seawater increase from 3.5 m/h at pH 8 to 7 m/h at pH 10.2, the latter representing the maximum value achieved within the full pH range studied. Subsequent increases in pH led to a sharp decline in settling rate, with values < 1 m/h observed near pH 11.

The corresponding results for synthetic tailings in a liquor containing only CaCl₂ displayed a steady increase in settling rate with pH across the entire range studied. In contrast, the settling rate trend for tailings prepared in the MgCl₂ liquor was almost identical to that found for the synthetic tailings in seawater. The results therefore indicate that the magnesium cation is the main species influencing flocculation performance for synthetic tailings suspensions in seawater. An increase in settling rate is observed between pH 9 and 10. Interestingly, this coincides with the zone of carbonate precipitate formation in seawater. The hydrolysis of Mg²⁺ and Ca²⁺ to MgOH⁺ and CaOH⁺ species, respectively, has been noted at pH 10, and adsorption of these complexes onto kaolin postulated as then reducing surface negativity (Avadiar et al., 2015); higher initial particle coagulation might then be a cause of higher settling rates on flocculation. Significantly, the observed sharp reduction of the settling rate coincides with the pH region in which the

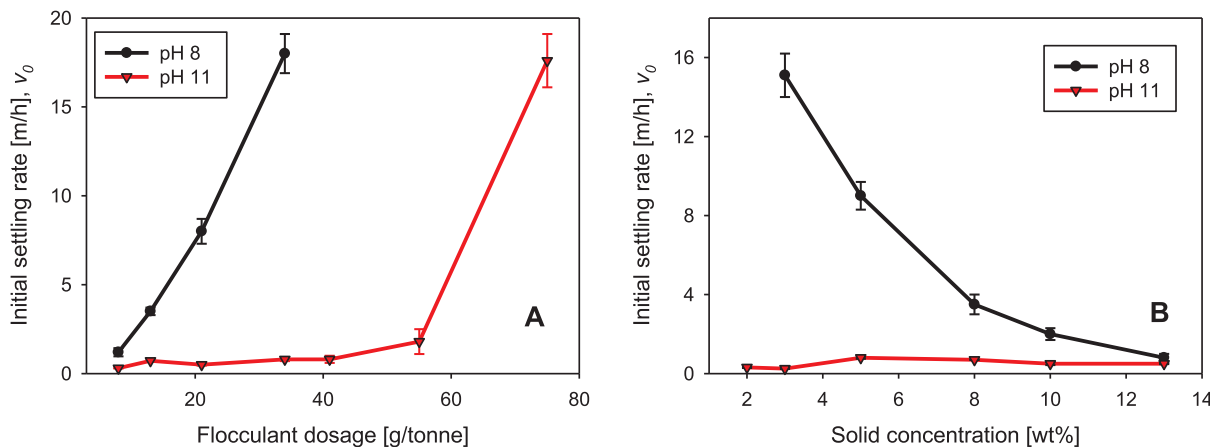


Fig. 7. Settling rate of synthetic tailings in seawater flocculated with HPAM. A: effect of flocculant dosage (solid concentration: 8 wt%), B: effect of solid concentrations (flocculant dosage 13 g/tonne).

buffer effect of seawater starts (Jeldres et al., 2019) and magnesium hydroxide precipitate formation is expected (El-Manharawy and Hafez, 2003; Jeldres et al., 2017a), and it is the formation of this phase which is likely to be responsible for inhibiting flocculation.

To gain further insights on the flocculation response in seawater, additional settling experiments were conducted in which flocculant dosage and solid concentrations were varied, focusing on pH 8 and 11. Fig. 7A shows the response to dosage at a solids concentration of 8 wt%, with the settling rate at pH 8 rising steadily from 1.2 to 18 m/h when the dosage was increased from 8 to 34 g/tonne. In contrast, much higher dosages were required before any enhancement of settling is observed at pH 11, with the settling rate remaining below 1 m/h up to a dosage of 34 g/tonne. Above a dosage of 55 g/tonne there was a significant elevation in settling rate to values comparable to those achieved at pH 8. That such high settling rates could be attained suggests that the inhibition of flocculation at the higher pH is not likely to be the consequence of flocculant deactivation, the prevention of flocculant adsorption or any change in aggregate structure that increases the extent of hindered settling; rather, it is consistent with the presence of an additional fine phase with a high surface area, which will be discussed further in Section 3.4.

The settling rate response as a function of solid concentration at a fixed dosage is shown in Fig. 7B. A very significant effect is observed at pH 8, with settling rates increasing substantially at higher solids dilution, a clear indication of the impact of hindered settling. The presence of clay within the synthetic tailings leads to the formation of highly porous aggregate structures as a consequence of edge-edge aggregation of the plate-like particles (Zhou and Gunter, 1992), and the growth of aggregates with such high effective volume fractions can be severely restricted at high solids concentrations. Even faster settling aggregates would be expected with further dilution below 3 wt%, although settling would then most likely be unhindered without an easily discernible interface.

The corresponding settling rates at pH 11 remained below 1 m/h over the entire synthetic tailings solids concentration range studied, confirming that hindered settling effects do not make a significant contribution to the sharp decline in settling rates at high pH. The formation of precipitates from magnesium present within seawater clearly adds additional fine particles to the suspension; while large aggregate sizes can still be achieved by applying much higher flocculant dosages, this is not a desirable option at an industrial scale and can have detrimental downstream implications (Bedell et al., 2015).

3.4. Flocculation kinetic of flocculated tailings in seawater

The dosage response curves shown in Fig. 7A imply an ‘induction’ region of low settling rates, after which higher dosages lead to a sharp elevation, and such trends have been frequently reported (Owen et al., 2007; Witham et al., 2012). In reality, some level of aggregation will be induced even at very low dosages, but the hindered settling rate for any aggregates formed is expected to be proportional to the size squared (Richardson and Zaki, 1954), and therefore the extent of aggregation can need to progress to moderate sizes before any shift in the settling response is observed. Kyoda et al. (2019) noted that FBRM offers much greater sensitivity to flocculation, showing the ‘induction’ region was absent in sizes derived from FBRM chord length distributions, with major increments in the volume-weighted chord length observed at much lower dosages.

An advantage of FBRM is the ability to monitor the extent of aggregation in real-time at a range of solids concentrations, which provides the scope to compare the kinetics of aggregate growth and breakage. Fig. 8 presents reaction profiles for the flocculation of 8 wt% synthetic tailings in seawater at different pH values for a fixed dosage of 13 g/tonne and under constant applied shear conditions. It can be seen

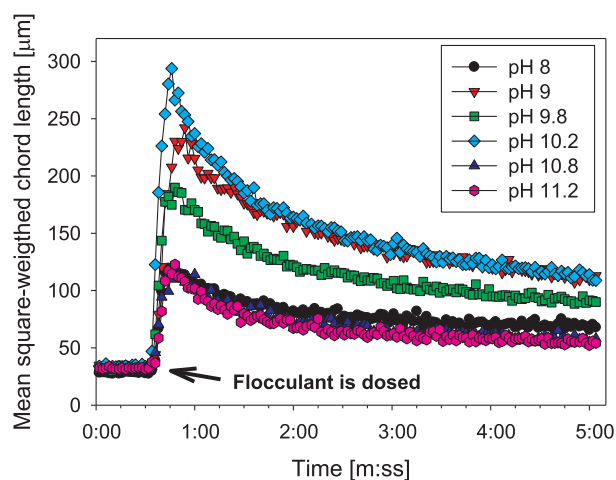


Fig. 8. Flocculation kinetic of synthetic tailings in seawater at different pH values (solid concentration 8 wt%, flocculant dosage 13 g/tonne, mixing at 150 rpm); pH adjusted with NaOH, with reported values representing stability achieved in measurements prior to flocculation.

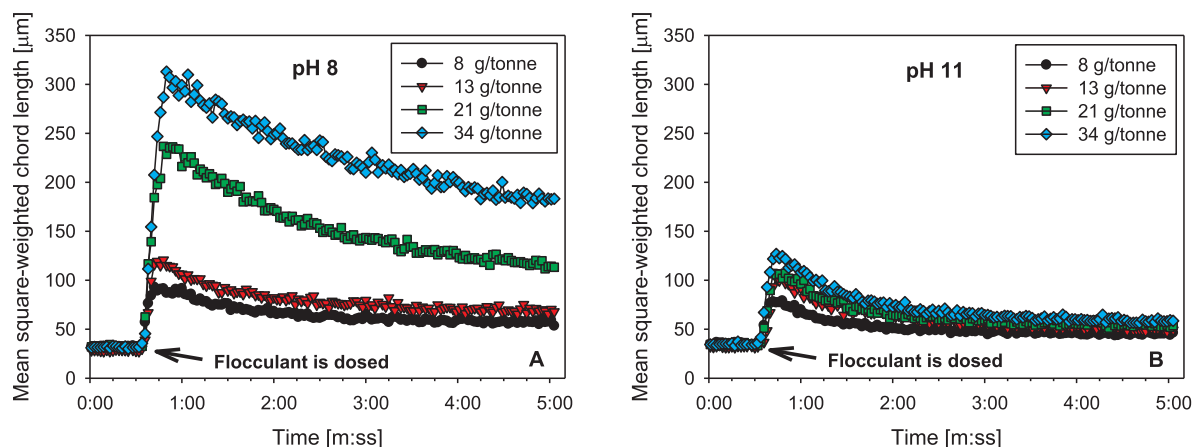


Fig. 9. Flocculation kinetic of synthetic tailings in seawater, showing the effect of flocculant dosage (solid concentration 8 wt%, mixing at 150 rpm). A: pH 8, B: pH 11.

that aggregate growth is very rapid after the flocculant is dosed, taking only a few seconds for the maximum aggregate size to be attained, but then fragmentation under the applied shear leads to a decay in the observed size until a plateau value is approached at extended reaction times. Similar to the sedimentation tests in seawater (Fig. 6), the kinetics of aggregate growth and breakage is pH-sensitive, with the largest aggregate size achieved at pH 10.2, while much smaller aggregates were exhibited at pH 8 and 11.

While the peak aggregate sizes seen at pH 8 and 11 in Fig. 8 were very similar, there appeared to be a greater degree of breakage after the peak and a lower plateau size at the higher pH, which may be indicative of a lower aggregate strength (Kirwan, 2009; Negro et al., 2005). To gain some insights into this behaviour, the flocculation response to variations in flocculant dosage (Fig. 9) and synthetic tailings solids concentration (Fig. 10) was examined at each pH. At pH 8 the system responded strongly to increments in dosage (Fig. 9A), the peak aggregate size increasing from 90 to ~300 μm over the dosage range from 8 to 34 g/tonne. In contrast, at pH 11 over the same dosage range (Fig. 9B), the peak aggregate size did not approach 150 μm, but even these small aggregates were prone to significant breakage at longer reaction times.

The presence of clays within a tailings suspension leads to flocculated aggregates of very high porosity, and as a consequence the flocculation response can be highly sensitive to solids concentration, with higher dilution favouring the formation of larger aggregates. Such behaviour is clearly evident for the synthetic tailings at pH 8 (Fig. 10A),

with a reduction in solids concentration to 5 wt% leading to a substantial increase in the peak aggregate size, and confirming that flocculation is not significantly inhibited at this pH. This was not the case at pH 11, for which the extent of aggregation remained limited at all three solids concentrations examined (Fig. 10B).

3.5. Images of aggregates formed in seawater

Cryo-SEM, in which cold stage SEM is applied following cryo-vitrification of flocculated clay structures and partial sublimation of vitrified water, has provided useful insights into the interactions between clay particle surfaces under different suspension conditions (Du et al., 2009; Zbik et al., 2008). However, the authors' claims of imaging low density, aggregate structures "directly" is questionable given the sampling and pre-treatment applied, particularly in view of the high shear sensitivity of such structures apparent in Fig. 8. Insertion of a PVM probe into a reaction vessel during flocculation provides the potential for direct imaging of aggregates in a suspension (Senaputra et al., 2014). This is clearly at a much lower magnification than cryo-SEM and without the ability to resolve individual particle interactions, but full aggregates of an industrially-relevant scale can be captured, as can the presence of other phases.

The formation of aggregates after flocculant dosing was captured directly through PVM in-situ imaging for 5 wt% synthetic tailings in seawater at pH 8. Fig. 11A presents a typical image of the unflocculated particle suspension, whereas Fig. 11B is for aggregates formed ~20 s

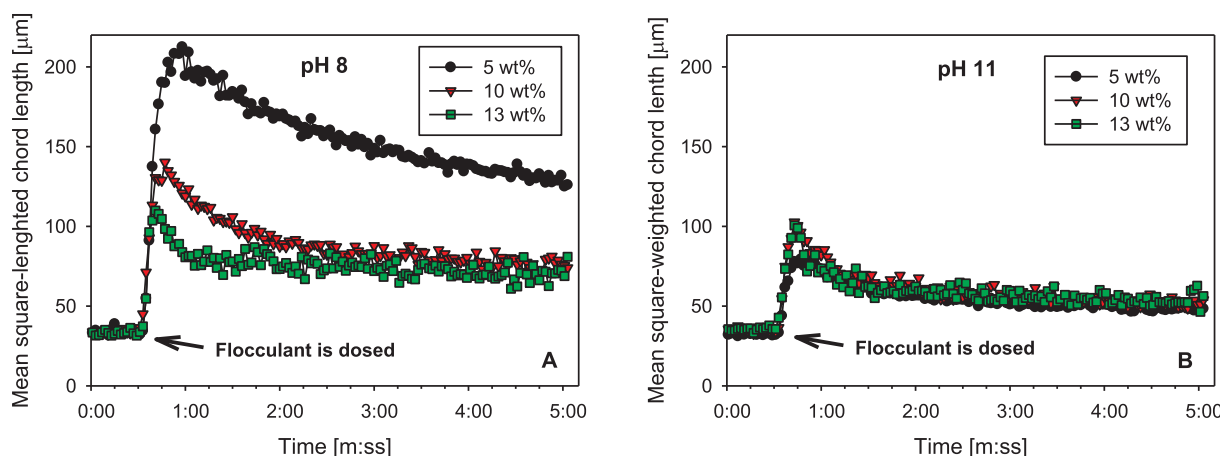


Fig. 10. Flocculation kinetic of synthetic tailings flocculated with 13 g/tonne HPAM in seawater at different solid concentrations. A: pH 8, B: pH 11.

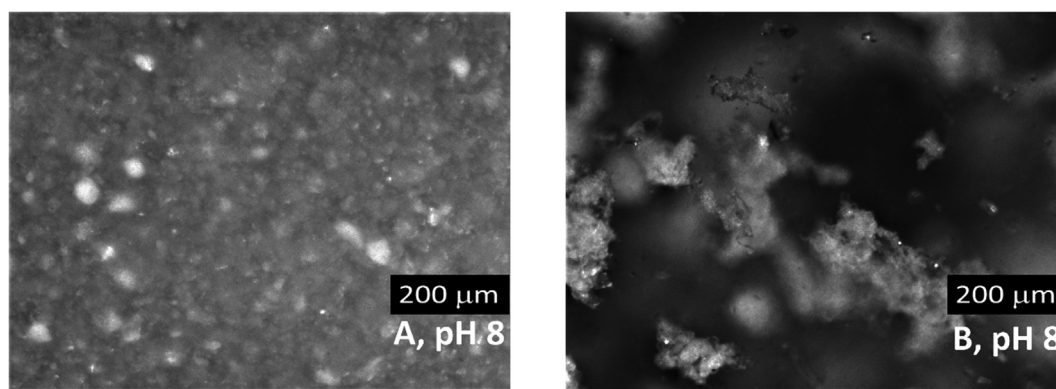


Fig. 11. PVM images of 5 wt% synthetic tailings in seawater at pH 8. A: unflocculated, B: flocculated with 13 g/tonne HPAM.

after dosing HPAM at 13 g/tonne. The unflocculated image indicates the presence of some larger particles, almost certainly from the quartz fraction, but the majority of the particles are at or below the resolution of the probe, even if partially coagulated, and in this state they cloud the appearance of the larger particles. On flocculation, all these fines are well captured into aggregates that are several hundred microns in size; co-flocculation with the coarser quartz particles is apparent. It is also worth noting the presence of large voids within the suspension after flocculation at this solids concentration, supporting the observation that larger aggregate sizes could be readily formed at higher dosages.

On raising the pH to 11, the suspension in an unflocculated state (Fig. 12A) does not appear noticeably different when compared with the lower pH, both images hinting at a degree of fine particle coagulation. The onset of aggregation can be seen after flocculant dosing (Fig. 12B), but the aggregates look far less resolved than at pH 8 (Fig. 11B). The main distinction between the flocculated images is the presence of quite hazy, possibly amorphous fines at pH 11 that are aggregated but potentially at a very high porosity. The voidage between aggregates is far less than at the lower pH, and this is also consistent with the expected precipitation of an additional phase.

3.6. Flocculation kinetic of flocculated tailings in CaCl_2 and MgCl_2 liquors

Fig. 13 presents the kinetics of aggregate growth and breakage at different pH values when dosing flocculant into synthetic tailings suspensions prepared in liquors containing Ca^{2+} or Mg^{2+} chlorides, representing the main divalent cations present within seawater. As expected, while flocculation in the presence of CaCl_2 results in a monotonic rise in aggregate size with increasing pH (Fig. 13A), the response in the presence of MgCl_2 exhibits an abrupt decline when the pH is above 10.2 (Fig. 13B), with the peak size then dropping from 230 μm to only 115 μm at pH 10.8. The observed trends are fully

consistent with the settling rate responses summarised in Section 3.3, where it was explained that the formation of solid magnesium hydroxide ($\text{Mg}(\text{OH})_2$) precipitates leads to a significant decline in the observed flocculation performance. In contrast, calcium hydroxide precipitates from the CaCl_2 brine would only form at a pH higher than 12, which is outside of the practical range of interest for the mining industry.

3.7. Calcium and magnesium precipitate interaction with flocculant

Further understanding of the impact of the precipitates formed at higher pH was gained by examining the three different saline liquors in the absence of the synthetic tailings solids, with turbidity measurements on the supernatants from cylinder settling then used to indicate the potential contribution to clarification issues. Tests were conducted both with and without flocculant addition to confirm if the solids are readily flocculated.

Independent of the liquor used, turbidity analysis shows insignificant values when the pH is below 10 (Fig. 14), consistent with the absence of any precipitate formation. However, $\text{Mg}(\text{OH})_2$ formation is observed at pH values > 10.3 in both seawater and 0.01 mol/L MgCl_2 liquors, leading the turbidity to increase as the pH is raised further. Solid precipitates of $\text{Ca}(\text{OH})_2$ only formed at pH values > 12 , which are outside of the experimental range of interest considered here.

The solid precipitates were readily flocculated and the supernatant turbidity after suspension settling returned to baseline values. While the $\text{Mg}(\text{OH})_2$ precipitates will likely contain a significant fraction of sub-micron solids, they will be coagulated at the high ionic strength, which is supported by the PSD shown in Fig. 5. As a consequence, the effective surface area of the solids exposed to flocculant will be substantially reduced, and as can be seen from Fig. 14, HPAM can effectively induce further aggregation even at high pH.

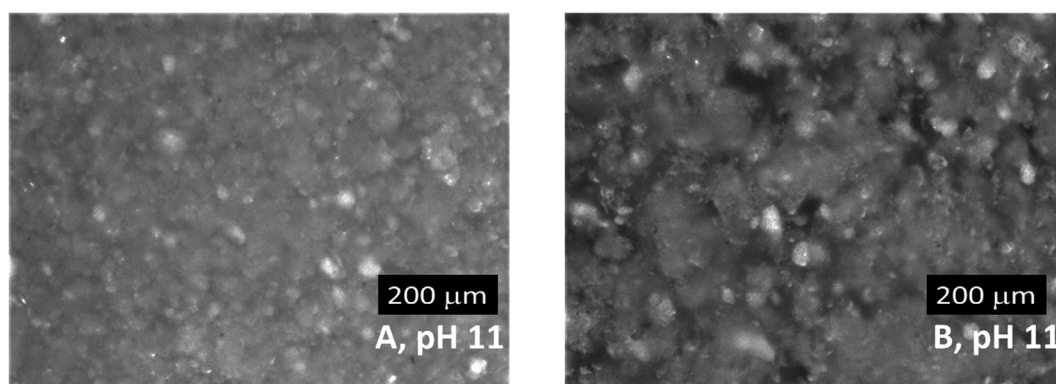


Fig. 12. PVM images of 5 wt% synthetic tailings in seawater at pH 11. A: unflocculated, B: flocculated with 13 g/tonne HPAM.

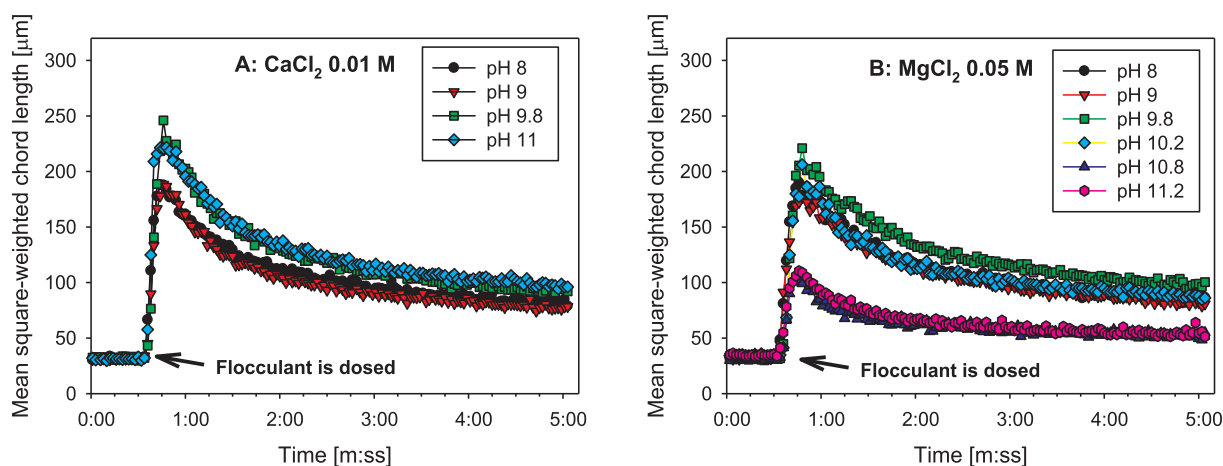


Fig. 13. Flocculation kinetic of 8 wt% synthetic tailing flocculated with 13 g/tonne HPAM in different aqueous media as a function of pH (solid concentration, flocculant dosage). A: 0.01 M CaCl_2 , B: 0.05 M MgCl_2 .

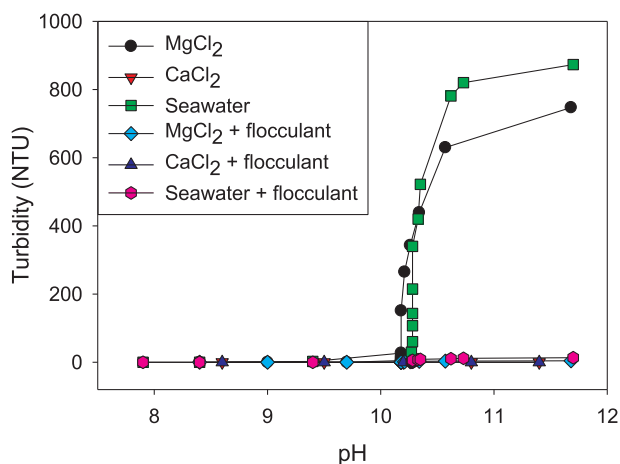


Fig. 14. Turbidity analysis of 0.01 mol/L Ca^{2+} , 0.05 mol/L Mg^{2+} , and seawater solutions with and without flocculant addition (measured 5 min after the commencement of settling).

4. Discussion

In the absence of flocculant, solid precipitates formed from solution Mg^{2+} under alkaline conditions for synthetic tailings in seawater favour mineral phase heterocoagulation. The unweighted FBRM chord length distributions (Fig. 4A) indicate that on raising the pH from 8 to 11, the fine particles coagulate to larger structures. From examination of the corresponding volume-weighted distributions (Fig. 4B), these additional coagulated structures are not larger than those that already existed in the suspensions at pH 8.

The high salinity of seawater causes the solution conformation of the anionic flocculant to contract, limiting its bridging capacity; however, the cations may form extra ionic bonds, which bridge the predominantly anionic particles and the anionic functionalities of the polymer (Jeldres et al., 2018; Quezada et al., 2018). This resulted in quite rapid settling rates being achieved at pH 8. While the reduced presence of ultrafine particles at pH 11 (illustrated in Fig. 4) might suggest that the tailings particles are more apt to interact with flocculant and form large aggregates (Semerjian and Ayoub, 2003), alkaline conditions actually led to poor flocculation performance and significantly reduced settling rates (Fig. 6). This phenomenon is undoubtedly associated with $\text{Mg}(\text{OH})_2$ precipitate formation at higher pH, but as shown in settling tests in the absence of the mineral phases

(Fig. 14), the precipitates themselves can be readily flocculated. However, the addition of the precipitated phase to the synthetic tailings still increases both the effective surface area exposed to flocculant and the number of particles or micro-aggregates that need to be further aggregated to attain acceptable settling rates. The dosage response at pH 11 (Fig. 7A) confirms this, showing that the onset of flocculation is inhibited in comparison to the low pH response, but above a threshold dosage, aggregation becomes effective and useful settling rates are then achieved. Unfortunately, such behaviour is only achieved at dosages that would be considered excessive for industrial purposes. For some feeds, this would also put higher demands on the need for solids dilution prior to flocculation.

The use of seawater in concentrator plants has been increasing within Chile (Cisternas and Gálvez, 2018). Although adequate settling performance can be achieved from tailings in high salinity environments, their efficiency in seawater is restricted to a pH range that does not promote the formation of divalent salt precipitates. It has been shown here that the presence of magnesium cations is primarily responsible for reducing flocculation efficiency and settling rates when it might otherwise be desirable to bring the operation to highly alkaline conditions (pH > 10).

This is of special relevance for the copper industry, where the minerals of interest are usually associated with large amounts of pyrite. The most favourable conditions for flotation of high pyrite minerals in fresh water are at pH values > 10.5, where flotation of the iron sulfide is depressed naturally. However, this strategy is not an option in seawater, not only because of implications to the recovery of byproducts such as molybdenum (Jeldres et al., 2017a) or the difficulty in raising the pH (Jeldres et al., 2017b), but also because tailings handling then becomes unsustainable. In this case, we recommend two alternatives that would benefit downstream tailings thickening operations: (i) work at a pH that avoids $\text{Mg}(\text{OH})_2$ precipitate formation, or (ii) treat the seawater to reduce its magnesium content before utilising it within the processing circuit.

5. Conclusions

A quartz-kaolin mixture was used as an analogue of industrial tailings from mineral processing. Its flocculation response was analysed over a range of pH values for suspensions in seawater and in liquors containing Ca^{2+} or Mg^{2+} , the main divalent cations present within seawater. The main conclusions were:

- Flocculation in seawater was found to be effective for pH < 10. Although salinity can limit the extent of aggregation by promoting coiling of the anionic polymer flocculant, there is also a positive

effect through the potential for solution cations to bridge between polymers and mineral surfaces.

- Flocculation performance was substantially impaired under highly alkaline conditions (pH > 10.3), with a sharp decline in settling rate to values < 1 m/h. It was demonstrated that this is due to the formation hydrolysed Mg²⁺ solid precipitates, which increases both the active surface area exposed to flocculant and the number of particles or micro-aggregates that need to be further aggregated to then attain acceptable settling rates. Settling tests from the flocculation of the saline liquors at high pH supported competition by such precipitates with the tailings mineral phases for flocculant adsorption.
- Flocculation in saline liquors and in particular seawater should not in itself be a significant problem for most thickening operations, but the generation of hydrolysed precipitates from divalent cations should be avoided, either by (i) operating upstream at a lower pH than may be otherwise ideal, or (ii) removing the magnesium content from seawater before it is used in mineral processing.

CRedit authorship contribution statement

Jahir J. Ramos: Data curation, Writing - review & editing. **Williams H. Leiva:** Data curation, Writing - review & editing. **Claudia N. Castillo:** Conceptualization, Formal analysis, Writing - original draft, Writing - review & editing. **Christian F. Ihle:** Formal analysis, Writing - review & editing. **Phillip D. Fawell:** Formal analysis, Writing - review & editing. **Ricardo I. Jeldres:** Conceptualization, Formal analysis, Writing - original draft, Writing - review & editing.

Declaration of Competing Interest

The authors declare that they have no known competing financial interests or personal relationships that could have appeared to influence the work reported in this paper.

Acknowledgements

RIJ is grateful for the support of CONICYT Fondecyt 11171036, CONICYT PIA ACM 170005 and the Centro CRHIAM Project Anid/Fondap/15130015. CFI acknowledges support from CONICYT Fondecyt Project No. 1160971 and CONICYT/PIA Project AFB180004.

References

- Atesok, G., Somasundaran, P., Morgan, L.J., 1988. Adsorption properties of Ca²⁺ on Na-kaolinite and its effect on flocculation using polyacrylamides. *Colloids Surf.* 32, 127–138. [https://doi.org/10.1016/0166-6622\(88\)80009-X](https://doi.org/10.1016/0166-6622(88)80009-X).
- Avadiar, L., Leong, Y.-K., Fourie, A., Nugraha, T., Clode, P.L., 2014. Source of Unimim kaolin rheological variation—Ca²⁺ concentration. *Colloids Surf. A Physicochem. Eng. Asp.* 459, 90–99. <https://doi.org/10.1016/j.colsurfa.2014.06.048>.
- Avadiar, L., Leong, Y.K., Fourie, A., 2015. Physicochemical behaviors of kaolin slurries with and without cations—Contributions of alumina and silica sheets. *Colloids Surf. A Physicochem. Eng. Asp.* 468, 103–113. <https://doi.org/10.1016/j.colsurfa.2014.12.019>.
- Bedell, D., Slottee, S., Shoenbrunn, F., Fawell, P., 2015. Thickening. In: Jewell, R.J., Fourie, A.B. (Eds.), *Paste and Thickening Tailings - A Guide*. Australian Centre for Geomechanics, Perth, pp. 113–136.
- Castillo, C., Ihle, C.F., Jeldres, R.I., 2019. Chemometric optimisation of a copper sulphide tailings flocculation process in the presence of clays. *Minerals* 9, 582. <https://doi.org/10.3390/min9100582>.
- Castro, S., 2018. The physico-chemical factors in flotation of Cu-Mo-Fe ores with seawater: a critical review. *Physicochem. Probl. Miner. Process.* 54, 1223–1236. <https://doi.org/10.5277/ppmp18162>.
- Cisternas, L.A., Gálvez, E.D., 2018. The use of seawater in mining. *Miner. Process. Extr. Metall. Rev.* 39, 18–33. <https://doi.org/10.1080/08827508.2017.1389729>.
- Costine, A., Cox, J., Travaglini, S., Lubansky, A., Fawell, P., Misslitz, H., 2018. Variations in the molecular weight response of anionic polyacrylamides under different flocculation conditions. *Chem. Eng. Sci.* 176, 127–138. <https://doi.org/10.1016/j.ces.2017.10.031>.
- Cruz, C., Reyes, A., Jeldres, R.I., Cisternas, L.A., Kraslawski, A., 2019. Using partial desalination treatment to improve the recovery of copper and molybdenum minerals in the Chilean mining industry. *Ind. Eng. Chem. Res.* <https://doi.org/10.1021/acs.iecr.9b00821>.
- Du, J., Pushkarova, R.A., Smart, R.S.C., 2009. A cryo-SEM study of aggregate and floc structure changes during clay settling and raking processes. *Int. J. Miner. Process.* 93, 66–72. <https://doi.org/10.1016/j.minpro.2009.06.004>.
- El-Manharawy, S., Hafez, A., 2003. Study of seawater alkalization as a promising RO pretreatment method. *Desalination* 153, 109–120. [https://doi.org/10.1016/S0011-9164\(02\)01110-4](https://doi.org/10.1016/S0011-9164(02)01110-4).
- Heath, A.R., Fawell, P.D., Bahri, P.A., Swift, J.D., 2002. Estimating average particle size by focused beam reflectance measurement (FBRM). *Part. Part. Syst. Charact.* 19, 84. [https://doi.org/10.1002/1521-4117\(200205\)19:2<84::AID-PPSC84>3.0.CO;2-1](https://doi.org/10.1002/1521-4117(200205)19:2<84::AID-PPSC84>3.0.CO;2-1).
- Hocking, M.B., Klimchuk, K.A., Lowen, S., 1999. Polymeric flocculants and flocculation. *J. Macromol. Sci. Part C Polym. Rev.* 39, 177–203. <https://doi.org/10.1081/MC-100101419>.
- Hogg, R., 1999. Polymer adsorption and flocculation. In: Laskowski, J.S. (Ed.), *Polymers in Mineral Processing*. Canadian Inst Min, Met & Petr., Canada, pp. 3–17.
- Ihle, C.F., Kracht, W., 2018. The relevance of water recirculation in large scale mineral processing plants with a remote water supply. *J. Clean. Prod.* 177, 34–51. <https://doi.org/10.1016/j.jclepro.2017.12.219>.
- Jeldres, M., Piceros, E., Robles, P.A., Toro, N., Jeldres, R.I., 2019. Viscoelasticity of quartz and kaolin slurries in seawater: Importance of magnesium precipitates. *Metals (Basel)* 9, 1120. <https://doi.org/10.3390/met9101120>.
- Jeldres, R.I., Arancibia-Bravo, M.P., Reyes, A., Aguirre, C.E., Cortes, L., Cisternas, L.A., 2017a. The impact of seawater with calcium and magnesium removal for the flotation of copper-molybdenum sulphide ores. *Miner. Eng.* 109, 10–13. <https://doi.org/10.1016/j.mineng.2017.02.003>.
- Jeldres, R.I., Calisaya, D., Cisternas, L.A., 2017b. An improved flotation test method and pyrite depression by an organic reagent during flotation in seawater. *J. South. African Inst. Min. Metall.* 117, 499–504. <https://doi.org/10.17159/2411-9717/2017/v117n5a12>.
- Jeldres, R.I., Forbes, L., Cisternas, L.A., 2016. Effect of seawater on sulfide ore flotation: A review. *Miner. Process. Extr. Metall. Rev.* 37, 369–384. <https://doi.org/10.1080/08827508.2016.1218871>.
- Jeldres, R.I., Piceros, E.C., Leiva, W.H., Toledo, P.G., Herrera, N., 2017c. Viscoelasticity and yielding properties of flocculated kaolinite sediments in saline water. *Colloids Surf. A Physicochem. Eng. Asp.* 529, 1009–1015. <https://doi.org/10.1016/j.colsurfa.2017.07.006>.
- Jeldres, R.I., Piceros, E.C., Wong, L., Leiva, W.H., Herrera, N., Toledo, P.G., 2018. Dynamic moduli of flocculated kaolinite sediments: effect of salinity, flocculant dose, and settling time. *Colloid Polym. Sci.* 296, 1935–1943. <https://doi.org/10.1007/s00396-018-4420-x>.
- Ji, Y., Lu, Q., Liu, Q., Zeng, H., 2013. Effect of solution salinity on settling of mineral tailings by polymer flocculants. *Colloids Surf. A Physicochem. Eng. Asp.* 430, 29–38. <https://doi.org/10.1016/j.colsurfa.2013.04.006>.
- Kaya, A., Yukselen, Y., 2005. Zeta potential of clay minerals and quartz contaminated by heavy metals. *Can. Geotech. J.* 42, 1280–1289. <https://doi.org/10.1139/t05-048>.
- Kirwan, L.J., 2009. Investigating bauxite residue flocculation by hydroxamate and polyacrylate flocculants utilising the focussed beam reflectance measurement probe. *Int. J. Miner. Process.* 90, 74–80. <https://doi.org/10.1016/j.minpro.2008.10.010>.
- Kyoda, Y., Costine, A.D., Fawell, P.D., Bellwood, J., Das, G.K., 2019. Using focused beam reflectance measurement (FBRM) to monitor aggregate structures formed in flocculated clay suspensions. *Miner. Eng.* 138, 148–160. <https://doi.org/10.1016/j.mineng.2019.04.045>.
- Lee, B.J., Schlautman, M.A., Toorman, E., Fettweis, M., 2012. Competition between kaolinite flocculation and stabilization in divalent cation solutions dosed with anionic polyacrylamides. *Water Res.* 46, 5696–5706. <https://doi.org/10.1016/j.watres.2012.07.056>.
- Li, W., Li, Y., Wei, Z., Xiao, Q., Song, S., 2018a. Fundamental studies of SHMP in reducing negative effects of divalent ions on molybdenite flotation. *Minerals* 8, 404. <https://doi.org/10.3390/min8090404>.
- Li, W., Li, Y., Xiao, Q., Wei, Z., Song, S., 2018b. The influencing mechanisms of sodium hexametaphosphate on chalcopryrite flotation in the presence of MgCl₂ and CaCl₂. *Minerals* 8, 150. <https://doi.org/10.3390/min8040150>.
- Li, Y., Li, W., Xiao, Q., He, N., Ren, Z., Lartey, C., Gerson, A., 2017. The influence of common monovalent and divalent chlorides on chalcopryrite flotation. *Minerals* 7, 111. <https://doi.org/10.3390/min7070111>.
- Liu, D., Edraki, M., Berry, L., 2018. Investigating the settling behaviour of saline tailing suspensions using kaolinite, bentonite, and illite clay minerals. *Powder Technol.* 326, 228–236. <https://doi.org/10.1016/j.powtec.2017.11.070>.
- Manukonda, V.R., Iwasaki, I., 1987. Control of calcium ion via chemical precipitation — ultrasonic treatment in selective flocculation. *Min. Metall. Explor.* 4, 217–222. <https://doi.org/10.1007/BF03402696>.
- Mpofu, P., Addai-Mensah, J., Ralston, J., 2003. Influence of hydrolyzable metal ions on the interfacial chemistry, particle interactions, and dewatering behavior of kaolinite dispersions. *J. Colloid Interface Sci.* 261, 349–359. [https://doi.org/10.1016/S0021-9797\(03\)00113-9](https://doi.org/10.1016/S0021-9797(03)00113-9).
- Negro, C., Fuente, E., Blanco, A., Tijero, J., 2005. Flocculation mechanism induced by phenolic resin/PEO and floc properties. *AIChE J.* 51, 1022–1031. <https://doi.org/10.1002/aic.10352>.
- Ordóñez, J.I., Moreno, L., Gálvez, E.D., Cisternas, L.A., 2013. Seawater leaching of caliche mineral in column experiments. *Hydrometallurgy* 139, 79–87. <https://doi.org/10.1016/j.hydromet.2013.07.009>.
- Owen, A.T., Fawell, P.D., Swift, J.D., 2007. The preparation and ageing of acrylamide/acrylate copolymer flocculant solutions. *Int. J. Miner. Process.* 84, 3–14. <https://doi.org/10.1016/j.minpro.2007.05.003>.
- Paredes, Á., Acuña, S.M., Toledo, P.G., 2019. AFM study of pyrite oxidation and xanthate adsorption in the presence of seawater salts. *Metals (Basel)* 9, 1177. <https://doi.org/10.3390/met9101177>.

- 10.3390/met9111177.
- Peng, F.F., Di, P., 1994. Effect of multivalent salts-calcium and aluminum on the flocculation of kaolin suspension with anionic polyacrylamide. *J. Colloid Interface Sci.* <https://doi.org/10.1006/jcis.1994.1161>.
- Quezada, G.R., Jeldres, R.I., Fawell, P.D., Toledo, P.G., 2018. Use of molecular dynamics to study the conformation of an anionic polyelectrolyte in saline medium and its adsorption on a quartz surface. *Miner. Eng.* 129, 102–105. <https://doi.org/10.1016/j.mineng.2018.09.025>.
- Richardson, J.F., Zaki, W.N., 1954. Sedimentation and fluidisation. Part 1. *Trans. Inst. Chem. Eng.* 32, 35–53.
- Romero, C.P., Jeldres, R.I., Quezada, G.R., Concha, F., Toledo, P.G., 2018. Zeta potential and viscosity of colloidal silica suspensions: Effect of seawater salts, pH, flocculant, and shear rate. *Colloids Surf. A Physicochem. Eng. Asp.* 538, 210–218. <https://doi.org/10.1016/j.colsurfa.2017.10.080>.
- Semerjian, L., Ayoub, G.M., 2003. High-pH–magnesium coagulation–flocculation in wastewater treatment. *Adv. Environ. Res.* 7, 389–403. [https://doi.org/10.1016/S1093-0191\(02\)00009-6](https://doi.org/10.1016/S1093-0191(02)00009-6).
- Senaputra, A., Jones, F., Fawell, P.D., Smith, P.G., 2014. Focused beam reflectance measurement for monitoring the extent and efficiency of flocculation in mineral systems. *AIChE J.* 60, 251–265. <https://doi.org/10.1002/aic.14256>.
- Spicer, P.T., Pratsinis, S.E., 1996. Shear-induced flocculation: The evolution of floc structure and the shape of the size distribution at steady state. *Water Res.* 30, 1049–1056. [https://doi.org/10.1016/0043-1354\(95\)00253-7](https://doi.org/10.1016/0043-1354(95)00253-7).
- Witham, M.I., Grabsch, A.F., Owen, A.T., Fawell, P.D., 2012. The effect of cations on the activity of anionic polyacrylamide flocculant solutions. *Int. J. Miner. Process.* 114–117, 51–62. <https://doi.org/10.1016/j.minpro.2012.10.007>.
- Zbik, M.S., Smart, R.S.C., Morris, G.E., 2008. Kaolinite flocculation structure. *J. Colloid Interface Sci.* 328, 73–80. <https://doi.org/10.1016/j.jcis.2008.08.063>.
- Zhou, Z., Gunter, W.D., 1992. The nature of the surface charge of kaolinite. *Clays Clay Miner.* 40, 365–368. <https://doi.org/10.1346/CCMN.1992.0400320>.